

lethal challenge. Although the toxicity of MDMA in mice is less consistent than in other species⁷, a 25% lethal dose (LD₂₅) is estimated as about 50 mg of drug per kg body weight⁸. Consistent with this, wild-type animals given increasing doses of MDMA under defined conditions succumbed within 4 h of drug administration, with one in five of the animals dying at a dose of 20 mg kg⁻¹ and three in ten dying at 40 mg kg⁻¹ (Fig. 2c). However, none of the UCP-3^{-/-} animals died after administration of either dose ($n = 5$ and $n = 10$, respectively).

Our results indicate that UCP-3 is required for the rise in skeletal and core temperature that is associated with MDMA administration. Endogenously produced reactive aldehydes can also stimulate UCP-3 activity⁹, and there are some structural similarities between this class of molecule and MDMA and/or its metabolites⁷. Further investigation is needed to determine whether ecstasy can directly stimulate uncoupling activity.

The temperature response in individuals who take excessive amounts of MDMA varies, and this variation could relate to the uncoupling activity of their skeletal muscle. For example, it is known that thyroid-hormone treatment can exacerbate the hyperthermic effects of amphetamines¹⁰ and that UCP-3 is upregulated by thyroid hormone¹¹. It is possible that UCP-2 and/or UCP-3 could also mediate the toxicity of agents such as ephedrine, methamphetamine and cocaine, recreational stimulants that can produce a similar hyperthermic response and which are related to MDMA. Our demonstration that UCP-3 is a molecular mediator of the thermogenic response to ecstasy suggests that agents designed to target uncoupling proteins could provide the basis for an important new therapeutic direction.

Edward M. Mills*, **Matthew L. Banks†**,
Jon E. Sprague†, **Toren Finkel***

*Cardiovascular Branch, NHLBI,
National Institutes of Health, Bethesda,
Maryland 20892-1622, USA

†Department of Pharmaceutical and Biomedical
Sciences, Ohio Northern University, Ada,
Ohio 45810, USA

e-mail: j-sprague@onu.edu

- Landry, M. J. *J. Psychoact. Drugs* **34**, 163–169 (2002).
- Dar, K. J. & McBrien, M. E. *Intensive Care Med.* **22**, 995–996 (1996).
- Lowell, B. B. & Spiegelman, B. M. *Nature* **404**, 652–660 (2000).
- Gong, D.-W. *et al. J. Biol. Chem.* **275**, 16251–16257 (2000).
- Vidal-Puig, A. *et al. J. Biol. Chem.* **275**, 16258–16266 (2000).
- Sprague, J. E., Banks, M. L., Cook, V. J. & Mills, E. M. *J. Pharm. Exp. Therap.* **305**, 159–166 (2003).
- Green, A. R. *et al. Pharm. Rev.* **55**, 463–508 (2003).
- Fantegrossi, W. E. *et al. Psychopharmacology* **166**, 202–211 (2003).
- Echtay, K. S. *et al. EMBO J.* **16**, 4103–4110 (2003).
- Halpern, B. N., Drudi-Baracco, C. & Bessirard, D. *Nature* **204**, 387–388 (1964).
- Gong, D. W., Karas, M. & Reitman, M. J. *J. Biol. Chem.* **272**, 241129–24132 (1997).

Competing financial interests: declared none.

Photonic crystals

Imaging by flat lens using negative refraction

The positive refractive index of conventional optical lenses means that they need curved surfaces to form an image, whereas a negative index of refraction allows a flat slab of a material to behave as a lens and focus electromagnetic waves to produce a real image¹. Here we demonstrate this unique feature of imaging by a flat lens, using the phenomenon of negative refraction in a photonic crystalline material. The key advance that enabled us to make this observation lies in the design of a photonic crystal^{2,3} with suitable dispersion characteristics to achieve negative refraction over a wide range of angles.

Although negative refraction has been demonstrated at microwave frequencies in a quasi-homogeneous metamaterial⁴, imaging by a flat lens is severely constrained because of large dissipation^{5,6} and anisotropy in the metamaterial. Plane-wave negative refraction at specific incident angles has been demonstrated at microwave frequencies by using a metallic photonic crystal prism⁷ and a dielectric photonic crystal⁸. However, to focus a diverging beam from a point source, the material must exhibit all-angle negative refraction² as well as low absorption.

Figure 1a shows the image of a microwave point source of frequency 9.3 GHz (wavelength, 3.22 cm) placed 2.25 cm from a two-dimensional flat lens made of a photonic crystal fabricated from an array of cylindrical alumina rods (see supplementary information). On the far side, a high-quality image is seen at a distance of 2.75 cm. Note that there is an image of similar size for the sub-wavelength source. This image is observed only in a narrow frequency range, between 9.0 and 9.4 GHz, with the best focus at 9.3 GHz. Outside this narrow band, at all other frequencies between 2 and 12 GHz, a single focus point is not seen.

These observations can be understood by examining the band structure of the photonic crystal and the corresponding equi-frequency surfaces, from which an effective refractive index, n_{eff} , can be defined and calculated⁹. In our geometry, the central axis of the diverging beam is along the (1,0) direction of the square lattice crystal. Just below the top of the second band, between 9.0 and 9.4 GHz, the equi-frequency surfaces move inwards with increasing frequency, consistent with negative n_{eff} . The condition for negative refraction, $n_{\text{eff}}(\theta) < 0$, holds for a diverging beam of sufficiently large angle, enabling the image to be formed. Figure 1 therefore also demonstrates wide-angle negative refraction by a photonic crystal.

The value of n_{eff} is necessarily angle-dependent. Inside the crystalline lens, the electromagnetic field is highly modulated and simple ray diagrams applicable in homogeneous media cannot be used. However, upon

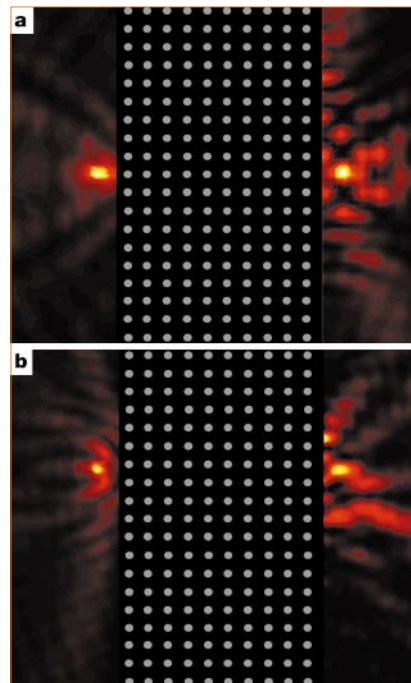


Figure 1 Imaging by a flat lens. **a**, Microwave electric-field-intensity map on a cross-sectional view of the two-dimensional source–image (left–right) system for the flat lens. **b**, Displacement of the image by 4 cm when the source is moved up by the same distance. Both panels correspond to dimensions of 37.5 × 30.0 cm. The intensity scale on the source side varies from –20 dB (yellow) to –48 dB (black), and on the image side from –30 dB to –75 dB.

emerging, the waves create a focus of the divergent beam emanating from the point object.

Conventional optical systems have a single optical axis and limited aperture, and cannot focus light onto an area smaller than a square wavelength¹. In contrast, our flat lens does not have a unique optical axis and is not restricted by aperture size. We have demonstrated both of these features by moving the source up by 4 cm: the image moves a corresponding distance in the same direction (Fig. 1b).

The unique properties of our flat lens provide new perspectives on imaging. A particular advantage of the photonic crystalline material is its scalability to submicrometre dimensions for possible applications from microwave to optical frequencies.

Patanjali V. Parimi, Wentao T. Lu, Plarenta Vodo, Srinivas Sridhar
Department of Physics and Electronic Materials
Research Institute, Northeastern University,
Boston, Massachusetts 02115, USA
e-mail: s.sridhar@neu.edu

- Pendry, J. B. *Phys. Rev. Lett.* **85**, 3966–3969 (2000).
- Luo, C. *et al. Phys. Rev. B* **65**, 201104(R) (4) (2002).
- Notomi, M. *Phys. Rev. B* **62**, 10696–10705 (2002).
- Shelby, R. A., Smith, D. R. & Schultz, S. *Science* **292**, 77–79 (2001).
- Houck, A. *et al. Phys. Rev. Lett.* **90**, 137401 (4) (2003).
- Iyer, A. K. *et al. Opt. Express* **11**, 696–708 (2003).
- Parimi, P. V. *et al. http://arxiv.org/abs/cond-mat/0306109* (2003).
- Cubukcu, E. *et al. Nature* **423**, 604–605 (2003).
- Foteinopoulou, S. & Soukoulis, C. M. *Phys. Rev. B* **67**, 235107(5) (2003).

Supplementary information accompanies this communication on Nature's website.

Competing financial interests: declared none.